



# Sulphur dioxide (SO<sub>2</sub>) vertical column density measurements by Pandora spectrometer over the Canadian oil sands

Vitali E. Fioletov<sup>1</sup>, Chris A. McLinden<sup>1</sup>, Alexander Cede<sup>2,3</sup>, Jonathan Davies<sup>1</sup>, Cristian Mihele<sup>1</sup>, Stoyka Netcheva<sup>1</sup>, Shao-Meng Li<sup>1</sup>, and Jason O'Brien<sup>1</sup>

- 5 <sup>1</sup>Environment Canada, Toronto, ON, Canada  
<sup>2</sup>NASA Goddard Space Flight Center, Greenbelt, MD USA  
<sup>3</sup>LuftBlick, Kreith, Austria

Correspondence to: Vitali E. Fioletov [vitali.fioletov@outlook.com](mailto:vitali.fioletov@outlook.com)

**Abstract.** Vertical column densities (VCDs) of SO<sub>2</sub> retrieved by a Pandora spectral sunphotometer at Fort McKay, Alberta, Canada, from 2013-2015 were analysed. The Fort McKay site is located in the Canadian oil sands region approximately 20 km north of two major SO<sub>2</sub> sources (upgraders) with total emission of about 45 kt yr<sup>-1</sup>. Elevated SO<sub>2</sub> VCD values were frequently recorded by the instrument with the highest values of about 9 DU (1 DU = 2.69•10<sup>16</sup> molecules•cm<sup>-2</sup>). Comparisons with co-located in-situ measurements demonstrated that there was a very good correlation between VCDs and surface concentrations in some cases, while in the others elevated VCDs did not correspond to high surface concentrations suggesting the plume was above the ground. Elevated VCDs and surface concentrations were observed when the wind direction was from south to southeast, i.e. from the direction of the two local SO<sub>2</sub> sources. The statistical error of the Pandora SO<sub>2</sub> VCDs from the spectral fitting uncertainty is under 0.05 DU for optimal observation conditions. The precision of the SO<sub>2</sub> measurements, estimated from parallel measurements by two Pandora instruments at Toronto, is 0.17 DU. The total uncertainty of Pandora SO<sub>2</sub> VCD, estimated using measurements when the wind direction was away from the sources, is under 0.26 DU (1-σ). Comparisons with integrated SO<sub>2</sub> profiles from concurrent aircraft measurements support these estimates.

## 1. Introduction

Sulphur dioxide (SO<sub>2</sub>) plays an important role in Earth's atmospheric chemistry and climate. It forms sulfate aerosols that influence weather and climate and leads to acid deposition through formation of sulfuric acid (H<sub>2</sub>SO<sub>4</sub>) (Hutchinson and Whitby, 1977). It is also a designated criteria air pollutant in many countries that poses a direct hazard to public health (Longo et al., 2010; Pope and Dockery, 2006). Active volcanoes are the primary natural source of SO<sub>2</sub>, while coal burning power plants, smelters, and oil refineries are the primary anthropogenic emitters of SO<sub>2</sub> into the atmosphere. In Canada, the majority of SO<sub>2</sub> emissions come from three sources: 32% from smelting and refining for non-ferrous metals, 22% from coal-fired electricity generation, and 21% from the petroleum industry (Wood, 2012). One of the largest sources of atmospheric pollutants, including SO<sub>2</sub>, in Canada is the oil sands operations. Located in the province of Alberta, the oil sands contain vast deposits of bitumen–oil mixed with sand, clay, and water. Environmental and health concerns associated with oil sands operations, including air



quality and acid deposition, are well known (Kelly et al., 2010). Highly elevated levels of SO<sub>2</sub> over the oil sands area have been detected there (Simpson et al., 2010) and are a subject of great concern. Due to the large size of the oil sands operation area, satellite measurements are an appealing approach for air pollution monitoring in this region.

The applications of satellites for monitoring SO<sub>2</sub> have been progressing rapidly during the last two decades. They are widely used to monitor volcanic (Carn et al., 2003, 2013; Fioletov et al., 2013; Krueger et al., 2000; Rix et al., 2012; Theys et al., 2013) and anthropogenic sources (Carn et al., 2007; Clarisse et al., 2011; Eisinger and Burrows, 1998; Fioletov et al., 2011, 2013; de Foy et al., 2009; Georgoulias et al., 2009; Lee et al., 2011; Nowlan et al., 2011; Thomas et al., 2005). More recently, satellites have been used for monitoring SO<sub>2</sub> (and NO<sub>2</sub>) emissions and trends in the oil sands region (McLinden et al., 2015, 2012, 2014). Many satellite instruments provide total column values (or vertical column densities, VCDs) but derivation of surface concentrations from them is not straightforward (Knepp et al., 2013). Ground-based measurements of the same quantity, VCD, help both in the validation of satellite measurements and facilitate a better interpretation of satellite data and their links to surface concentration (Richter et al., 2013).

Ground-based observations of SO<sub>2</sub> VCDs were first made by Brewer spectrophotometers, using the strong absorption features of SO<sub>2</sub> in the ultraviolet (UV) part of the spectrum (Kerr et al., 1988). The Brewer spectrophotometer operating in the Direct Sun (DS) mode measures UV at 5 wavelengths between 306 and 320 nm to retrieve column ozone and SO<sub>2</sub>. Such measurements have been used to monitor volcanic SO<sub>2</sub> (Krueger et al., 1995) and anthropogenic SO<sub>2</sub> in extreme pollution events (De Backer and Muer, 1991; Zerefos et al., 2000). The uncertainty of the Brewer DS SO<sub>2</sub> measurements is about 1-2 Dobson Units (DU, where 1 DU is equal to  $2.69 \cdot 10^{16}$  molecules $\cdot$ cm<sup>-2</sup>) and is typically insufficient for air quality applications. A Brewer can also measure global spectral UV irradiance on a horizontal surface in the spectral range 290-325 nm or 286-363 nm (depending on the modification) with 0.5 nm increment. Pronounced SO<sub>2</sub> absorption features were seen in these global UV spectra when SO<sub>2</sub> amounts were high (Bais et al., 1993). SO<sub>2</sub> VCD can be even derived from such global spectral UV measurements (Fioletov et al., 1998). However this method of SO<sub>2</sub> VCD retrieval is less sensitive than the Brewer DS method and has the detection limit of about 5 DU. A more accurate method (with an uncertainty as low as 0.13 DU) based on Brewer “group-scan” spectral direct sun radiation measurements at 45 wavelengths from 306 nm to 324 nm was developed (Kerr, 2002), but not widely implemented due to its complexity.

Ground-based multi-axis differential optical absorption spectroscopy (MAX-DOAS) method is another technique used for ground-based SO<sub>2</sub> retrievals. The method is based on scattered sunlight measured in the visible and UV part of the spectrum at different elevation angles with data analyzed using the DOAS technique (Platt and Stutz, 2008). In addition to total VCD, the method can provide some information on the vertical profile. It was widely used for measurements of volcanic SO<sub>2</sub> under the Network for Observation of Volcanic and Atmospheric Change (NOVAC) project (Galle et al., 2010). Only a few studies have focused on MAX-DOAS measurements of anthropogenic SO<sub>2</sub> (Wang et al., 2014; Wu et al., 2013). The uncertainty of the retrieved SO<sub>2</sub> estimated from the spectral fitting error is about 0.1 DU (Wang et al., 2014).



Pandora (SciGlob, <http://www.sciglob.com/>) is a recently developed instrument for UV and visible spectral measurements which was primarily designed for direct-sun observations, but is also capable of conducting zenith sky (ZS) and MAX-DOAS measurements. Similar to the Brewer instrument, it tracks the Sun, but as it measures the entire spectrum at once, a DOAS-type algorithm can be applied. The instruments were used in several NASA Deriving Information on Surface  
5 Conditions from Column and Vertically Resolved Observations Relevant to Air Quality (DISCOVER-AQ) campaigns. DISCOVER-AQ is a series of field missions with an overarching objective to improve the interpretation of satellite observations to diagnose near-surface conditions relating to air quality (Reed et al., 2013). It has been demonstrated that Pandora can successfully measure total column ozone and NO<sub>2</sub> (Herman et al., 2009, 2015; Tzortziou et al., 2012, 2013). The instrument characteristics are suitable for total column SO<sub>2</sub> measurements, but available information on Pandora SO<sub>2</sub>  
10 measurements is very limited (Knepp et al., 2013). This is probably a result of most Pandora instruments being deployed away from major SO<sub>2</sub> sources. In 2013, a Pandora instrument, along with other instrumentation, was deployed to the oil sands region where relatively high SO<sub>2</sub> column amounts are common (McLinden et al., 2012; Simpson et al., 2010). This made it possible to establish optimal retrieval procedures for the Pandora SO<sub>2</sub> measurements, estimate uncertainties, and study the relationship between total columns and surface concentrations.

## 15 2. Instruments and Locations

The Pandora spectrometer system is based on an Avantes symmetric Czerny-Turner optical bench design with a 2048 CCD linear array detector. The Pandora spectrometer system consists of an optical head sensor, mounted on a computer controlled sun-tracker and sky-scanner, and connected to an Avantes array spectrometer by means of a 400-micron core diameter single strand multi-mode optical fiber. It operates in the 280-530 nm spectral range with a 0.6 nm slit function width. A detailed  
20 description of the instrument is given by (Herman et al., 2009). Wavelength calibration and slit functions for Pandora instruments were determined by the manufacturer from lamp emission lines (Hg, Cd, Cu, In, Mg, Zn). Wavelength stability is validated during instrument operation by an analysis of the solar Fraunhofer line structures. Stray light in the 304 to 330 nm range (used for SO<sub>2</sub> retrievals) is reduced by utilizing a U340 (280–380 nm) band pass filter with cut-off at 380 nm. Further stray light correction is obtained from pixels corresponding to 280 to 285 nm, which contain almost zero direct illumination.  
25 We used the instrument in DS and ZS modes but will limit this study to DS measurements only. To allow for the detection of different absorbers, the instrument periodically measures UV spectra with the U340 filter on and off, with the interval of about 90 seconds.

In 2013, Environment Canada (EC) acquired two Pandora sun spectrometers from SciGlob. One of them, with Serial Number 104, after a 3-week testing period at Toronto, was deployed to Fort McKay (57.184°N, 111.64°W) in the oil sands  
30 region, where it began operations on August 15, 2013. The instrument head was mounted on a tripod and the spectrometer and computer were installed in a water-proof plastic housing (Figure 1, left). The head and the housing were connected by 10 m-long optical, data and power cables. Such configuration provided a rapid deployment of the instrument, but it could not



withstand a cold Alberta winter. The instrument was shipped back to Toronto on December 3, 2013. It was then redeployed on August 21, 2014 in a different configuration with the instrument head installed on the roof of the EC instrument trailer, while the spectrometer and computer were installed inside the trailer in a temperature-controlled environment (Figure 1, right).

The site at Fort McKay is equipped with various instruments for air quality measurements. In this study, we used the in situ measurements of SO<sub>2</sub> as well as the wind speed and direction data provided by Recordum Airpointer© suite of instruments (<http://recordum.eu/recordum-airpointer/>). According to the manufacturer, the precision of SO<sub>2</sub> measurements is about 1 ppb. The Airpointer reports data with a 1-minute time resolution. We used 10-minute averages matched with 10-minute averaged Pandora data.

Fort McKay is a small town (population of 600) surrounded by five oil sands surface mining facilities to the north and south. There are two major SO<sub>2</sub> sources located south of Fort McKay: the Syncrude Mildred Lake plant is located 16 km to the south of Fort McKay and the Suncor Millennium Plant 23 km south-south-east. According to the National Pollutant Release Inventory (NPRI, <http://www.ec.gc.ca/inrp-npri>), the 2014 annual emissions were about 26 kt and 17 kt of SO<sub>2</sub> per year from the Syncrude and Suncor facilities, respectively. There is also a source (Horizon Oil Sands processing plant and mine) 18 km north, but the emission from that source are only 4 kt per year. There are hundreds of kilometres of pristine boreal forests to the west and east from Fort McKay with no SO<sub>2</sub> sources. Thus, the pollution level at Fort McKay is largely dependent on the wind direction.

Another Pandora instrument (S/N 103) was installed October 14, 2013 on the roof of the EC building at Downsview (43.782°N, 79.47°W), a typical urban location in Toronto. The instrument head was mounted on a tripod, but the spectrometer and computer were located inside the building and connected to the head by a 10 m cables. The same configuration was used for Pandora 104 when the instrument was in Toronto. The two instruments were run side-by-side from January to June 2014 making a direct comparison possible. According to NPRI, there are no large SO<sub>2</sub> emission point sources in the vicinity of the EC building in Toronto, but there are multiple sources with emissions under 10 kt per year in the area. The largest source with total emissions of about 12 kt per year is a cluster of plants on the west coast of Lake Ontario about 60 km from the site.

### 3. Pandora's SO<sub>2</sub> Algorithm and Data.

The Pandora Operation and Analysis Software Suite (Version 1.6, available from <http://avdc.gsfc.nasa.gov/pub/tools/Pandora/install/>) was used for data processing and retrieval. The software can be configured to include a specific set of retrieved species and to use an extraterrestrial reference spectrum, etc. The information about the retrieval algorithm and configuration settings is available from the software manual. In particular, the software allows for the selection of a spectral fitting window. MAX-DOAS retrievals tend to use narrow spectral windows to avoid differences in the air mass factors ( $\mu$ ) for individual wavelengths within the window caused by differences in optical paths due to scattering. This factor is far less important for DS measurements.



The first step in the Pandora spectral fitting algorithm is to subtract the irradiance logarithm of the measured spectra from the irradiance logarithm of the reference spectrum. Then, a simultaneous least-squares fit is applied to the difference between measured and reference spectra (see (Herman et al., 2009) for details) as illustrated by Figure 2. The fitted functions are a low-order polynomial, the absorption spectra of SO<sub>2</sub> and other atmospheric absorbers, and wavelength shift and squeeze  
5 functions.

The Pandora standard algorithm uses a SO<sub>2</sub> absorption cross section at 295 K (Vandaele et al., 1994) in the retrieval. As the SO<sub>2</sub> absorption cross section possesses very distinct absorption features (Figure 3a), a wider fitting window, including more spectral lines, should reduce the uncertainties of the retrievals. Figure 3 also shows SO<sub>2</sub> values retrieved for the 304-311 nm, 311-330 nm, 304-330 nm, and 306-330 nm spectral windows based on measurements taken at Fort McKay on September  
10 14, 2013 (Figure 3c, and at Downsview on March 16, 2014 for both instruments (Figures 3b and 3d). It is evident from the plot that the first two windows produce SO<sub>2</sub> values that have a much larger scattering than the values retrieval based on the entire 304-330 nm spectral window. The SO<sub>2</sub> absorption spectrum has strong peaks in the 304-311 nm spectral window, but the absolute signal is weaker and the stray light is higher than in the 311-330 nm spectral window. However the weaker SO<sub>2</sub> absorption features in 311-330 nm result in increased sensitivity to the influence of ozone and possibly other absorbers.

The 306-330 nm spectral window was used in this study. When SO<sub>2</sub> is high, the values retrieved using all 4 spectral windows are very similar. The retrievals using the 306-330 nm spectral window are nearly identical to those obtained for the 304-330 nm window, but produce slightly lower uncertainties. The software also has the option to use a prescribed extraterrestrial spectrum or to generate it from the measurements (“synthetic reference spectrum”). Both options were tested and the latter option was used as it produces slightly smaller uncertainties. Note that the synthetic reference spectrum was  
15 established from clear sky measurements in Toronto before each instrument deployment to Fort McKay and then used to process all subsequent data.

Several criteria were used for data filtering. The instrument integration time varies from 4 to 4000 ms depending on the signal strength. To exclude measurements when the Sun was covered by clouds, a 500 ms cut-off limit was used as a quality control tool: measurements that required more than 500 ms integration time were rejected. Furthermore, for high Sun elevations  
25 lower cut-off limits were used: 300 ms for airmass ( $\mu$ ) value  $\mu < 3$  and 100 ms for  $\mu < 2$ . Measurements taken at  $\mu > 5$  were not used. In addition to SO<sub>2</sub> vertical column calculation, the Pandora data processing software calculates its statistical uncertainty. After the filtration by the integration time, the statistical fitting uncertainties are less than 0.05 DU for 60%, and between 0.05 DU and 0.15 DU for about 30%, of all retrieved VCD values. Higher uncertainty values are related to measurements at low Sun position or under very thin clouds. Only data with a fitting uncertainty of SO<sub>2</sub> VCD  $< 0.35$  DU were used.

We encountered one practical problem related to the fitting algorithm that appears when the SO<sub>2</sub> amount is close to zero and the measurements are relatively noisy (e.g. due to thin clouds). On some occasions, the fitting algorithm finds the best fit with a small wavelength offset and an artificially elevated (by as much as 1 DU) SO<sub>2</sub> value. Only 2-3% of the data are affected by this error, but they are very noticeable on time series plots. A simple filtering by the standard error of retrieved SO<sub>2</sub> and/or by the wavelength offset removes these erroneous data, but it can also remove some valid observations. As  
30



mentioned, there are two options for the reference spectrum: an independently measured extraterrestrial spectrum (“prescribed reference spectrum”) or generated from the measurements themselves (“synthetic reference spectrum”). Such problematic cases were processed with the prescribed spectrum that appear to give better results in this situation than processing with the synthetic reference spectrum used for all other retrievals.

5           The calibration procedure for NO<sub>2</sub> DS DOAS measurements (determining the absolute slant column amount in the reference spectrum) is described by Herman et al. (2009). It is based on a linear fit of the lowest 2% (or so) slant column values as a function of the air mass. Unlike NO<sub>2</sub> measurements with a precision of 0.01 DU (Herman et al., 2009), retrievals of SO<sub>2</sub> have to deal with relatively high noise in individual measurements, their precision is about 0.17 DU (shown later). This means that 2<sup>nd</sup> percentile will be determined largely by the noise and not the lowest VCD values. Also, unlike stratospheric NO<sub>2</sub> that  
10 is always present in any NO<sub>2</sub> VCD retrieval, we can assume that there is a certain fraction of measurements without any measurable SO<sub>2</sub> presence in the atmosphere. We modified the NO<sub>2</sub> calibration approaches to make it more suitable for SO<sub>2</sub> by considering higher percentiles and then adjusting the “baseline” level using known characteristics of the noise distribution function as described below.

15           Figure 4 (top) shows slant column SO<sub>2</sub> measured at Fort McKay in August-September 2013 as a function of the air mass factor  $\mu$ . In the absence of any SO<sub>2</sub>, the slant column values should be scattered around the zero line, so the mean and median values as a function  $\mu$  of should be equal to zero. If, however, the reference spectrum is not absolutely correct, it may contain structures that the fitting procedure interprets as a contribution from SO<sub>2</sub> absorption. Similarly, if the ozone absorption is not accounted for completely, the fitting procedure could produce a residual SO<sub>2</sub> signal that depends on  $\mu$ . Thus, even in  
20 the case with no SO<sub>2</sub> in the atmosphere, the mean (or median) value of slant column are not constant, but can be described as a linear function (in the simplest case) of  $\mu$ . That function could be used as a reference corresponding to zero SO<sub>2</sub> slant column values in the SO<sub>2</sub>-free atmosphere.

25           If we assume that SO<sub>2</sub> is present even in a fraction of all observations at an otherwise SO<sub>2</sub>-free site, then the mean value will be elevated compared to the SO<sub>2</sub>-free “clean” atmosphere and therefore it cannot be used as a reference in the calibration procedure. However, the low percentiles (e.g., 5<sup>th</sup>, 10<sup>th</sup> or 25<sup>th</sup>) of slant column values are close to the same percentiles for “clean” conditions making them more suitable for determining the absolute slant column amount in the reference spectrum. There are two potential complications: first, the low percentiles could be biased low relative to zero SO<sub>2</sub> conditions due to random errors, thereby resulting in scattering of data points. The lower the percentile value, the larger that bias. Second, the standard deviation of the scattering increases with the air mass factor as the signal strength declines resulting in higher errors and lower values in the low percentiles.

30           The intercept ( $a$ ) and slope ( $b$ ) of different percentile lines were determined by a method that is based on quintile regressions (Koenker and Bassett, 1978). Once the slope and intercept of the reference line are known, the VCD values can be derived from Slant Column Density (SCD) as  $VCD = (SCD - a) / \mu - b$ . This selection of a particular percentile line as a reference introduces a bias that can be corrected using the information about measurement uncertainties as discussed below. We used





the 25<sup>th</sup> percentile in our calculations. Note that the distances between the 25<sup>th</sup> percentile and 50<sup>th</sup> or 10<sup>th</sup> percentiles for VCDs are +0.16 DU and -0.12 DU respectively.

The fact that the slope of the regression line for the SCD versus  $\mu$  in the absence of SO<sub>2</sub> is negative may seem counterintuitive, but the spectral fitting procedure is dominated by the ozone signal. A small imperfection in accounting for ozone absorption can be compensated by a biased SO<sub>2</sub> signal. As the shape of the ozone profile and the temperature of the ozone layer are changing throughout the year, this calibration procedure was applied on a monthly basis. The correction to the VCD (that is equal to  $-a/\mu-b$ ) introduced by this calibration procedure is not negligible and changes throughout the year. For  $\mu=3$ , the correction value ranges from -0.15 DU in October to 0.55 DU in May.

Estimation of the instrument precision would be an easy task if we could install the instrument in an SO<sub>2</sub>-free location, but this was not the case for our sites. However, the side by side operation of two instruments at Toronto made it possible to study the precision of Pandora's SO<sub>2</sub> measurements. Figure 5 shows a scatter plot of the SO<sub>2</sub> values by the two instruments from January 16, 2014 to July 31, 2014 when both instruments were at the Downsview site. Typically, the SO<sub>2</sub> VCD values in Toronto are relatively small, less than 1.7 DU. The correlation coefficient between the measurements of the two instruments shown in Figure 5 is 0.7. Using Grubbs estimation method (see Appendix 1 for details) and assuming that there is no multiplicative bias between measurements we can calculate that the standard deviations of instrument errors are 0.18 and 0.16 DU for Pandora 103 and 104 respectively.

This information about the instrument errors can be used to reduce the effect of an arbitrary selection of the percentile line as a reference used by the calibration procedure. If we assume that the instrumental errors have a Gaussian distribution with a 0.17 DU standard deviation, then in the absence of any SO<sub>2</sub> the 25<sup>th</sup> and 10<sup>th</sup> percentile values would be -0.11 DU and -0.22 DU respectively. These values represent the biases introduced by the calibration procedure and should be added back to the retrieved values. Note that the lower the percentile value, the less the calibration procedure is affected by non-zero SO<sub>2</sub> values. However, the lower the percentile value, the higher the uncertainty of the percentile estimate and the higher the impact of the uncertainty of the instrumental error estimate can have on the size of the bias. In our case, either the 25<sup>th</sup> or 10<sup>th</sup> percentile seems to be optimal. As the distance between them from the Gaussian distribution with  $\sigma=0.17$  DU is -0.11 DU, very close to the -0.12 DU value from the Figure 4 (bottom) estimates, there is no impact on the results regardless of what percentile value to use.

The precision of Pandora instruments is high and the two instruments track each other very well, but there could be systematic errors related to the retrieval algorithm itself. Figure 3b and d shows an extreme example when both instruments reported fluctuations around the zero line with negative values as low as -0.4 DU. Column ozone was high on that day (420 DU) and the incomplete removal of ozone absorption features by the spectral fitting algorithm could be a possible explanation for such a large negative value. The SO<sub>2</sub> values retrieved using the 304-311 nm spectral window, where the influence of other absorbers is smaller due to the stronger SO<sub>2</sub> absorbing features, are close to the zero line. Similar fluctuations with positive and negative values at Fort McKay were observed on days when surface concentrations were close to zero with the site at



upwind of the sources, indicating these fluctuations were not related to real changes in SO<sub>2</sub> VCD. Further improvement of the retrieval algorithm could increase the accuracy of Pandora's SO<sub>2</sub> measurements.

#### 4. SO<sub>2</sub> Measurements at Fort McKay

The site at Fort McKay is located 20 km from the major emission sources and SO<sub>2</sub> values as high as 9 DU are observed from time to time. Time series of SO<sub>2</sub> measurements at Fort McKay in August 2013 – October 2015 are shown in Figure 6. Different colours and symbols represent different uncertainties of the retrieved values as estimated by the Pandora processing software.

The first days of the Pandora operation at Fort McKay revealed that a combination of strong emissions from the industrial sources to the south with southern winds result in “pollution events” characterized with high VCD values of SO<sub>2</sub> and NO<sub>2</sub>. An example of such an event on August 23, 2013 is shown in Figure 7a. During that event, the wind direction was from the south or southeast, i.e. from the direction of the major pollution sources.

Although the VCD and surface concentration are different quantities, they are often affected by the same plume and therefore correlated. In situ measurements on August 23, 2013, demonstrated the same behaviour of surface SO<sub>2</sub> and VCDs as illustrated by Figure 7a with a relationship where each 10 ppbv at the surface corresponds to about 1 DU in total column. However, this column-surface relationship is different from event to event. Figures 7b and 7c show examples of pollution events on November 4 and 5, 2013, when 1 DU corresponds to about 5 ppbv and 20 ppbv respectively. On some occasions, the VCD and surface concentration show a similar behaviour for many hours (Figure 7d), while on other days the changes in surface concentration follow the VCD changes with some time lag (Figure 7e) probably due to the shape of the plume, or do not really show any good correlation (Figure 7f). In the case of August 2, 2015 (Figure 7f), the SO<sub>2</sub> plume was above the ground early in the morning and was not detected by in-situ instruments.

High surface concentrations should contribute to elevated vertical columns. The examples presented above indicate that the opposite may not be always true: Elevated vertical column densities may be related to plumes that are above the ground and therefore may not produce high surface concentrations. This is further illustrated by Figure 8 where scatter plots of surface concentrations binned by VCD values and VCDs binned by surface concentrations are shown.

Surface wind data were used to study the dependence of VCDs and surface concentrations on wind directions. The main SO<sub>2</sub> emission sources are located within about 20 km to the south of Fort McKay, and the winds from the south generally produce elevated SO<sub>2</sub> values. Figure 9a confirms that surface SO<sub>2</sub> concentrations are the highest when the wind direction is south-southeasterly. This can be seen for both the mean values and for extremes (90<sup>th</sup> percentile).

As discussed in Section 3, the calibration procedure is based on the assumption that a certain fraction of all measurements corresponds to “clean” conditions. As Figure 9a shows, surface concentrations are very low for most wind directions except south and south-east. This can be used to refine the calibration-related bias in Pandora data mentioned in Section 3. A minimum in SO<sub>2</sub> of about zero was found for winds from the west as expected from the location of industrial





sources. We can assume that this direction represents clean conditions and this gives us an additional confidence in the suggested calibration procedure. Figure 9b shows Pandora SO<sub>2</sub> VCD as a function of the wind direction with this bias removed. As expected, it is very similar to the distribution of surface concentrations from Figure 9a.

It should be noted that the 90<sup>th</sup> percentile values for the direction from west are 0.25-0.3 DU (Figure 9b). This can be interpreted as yet another estimate of the overall uncertainty of Pandora's SO<sub>2</sub> data. If we assume the Gaussian distribution of the errors, then the 0.3 DU value of the 90<sup>th</sup> percentile corresponds to 0.23 DU value of the standard deviation. The standard deviation as calculated directly is between 0.22 and 0.26 DU for six 10-degree bins corresponding "clean" western directions. These values are higher than the previously estimated 0.17 DU value of the instrument precision, but they also include the errors related to imperfection of the retrieval algorithm.

Aircraft-based measurements of air pollutants from sources in the Canadian oil sands were made in support of the Joint Canada–Alberta Implementation Plan for Oil Sands Monitoring during a summer intensive field campaign between 13 August and 7 September 2013 (Gordon et al., 2015). The SO<sub>2</sub> measurements from these flights were used to examine the accuracy of the Pandora VCDs. Specifically, 7 spirals were flown within 4 km of Fort McKay in which vertical profiles were made with a Thermo Scientific 43i-TLE analyser. The measured vertical profiles of SO<sub>2</sub> mixing ratios and the wind directions as a function of altitude for these 7 flights are shown in Figure 10. Integrated SO<sub>2</sub> columns were compared with Pandora VCDs and the results are shown in Figure 11 and Table 1. The minimum altitude range flown by the aircraft used to construct a profile was 100-1500 m, with most profiles exceeding 2000 m. The integrals were calculated for two scenarios for SO<sub>2</sub> concentrations below the lowest aircraft flight altitude of about 100-150 m: assuming a zero mixing ratio between the ground and the lowest aircraft altitude, and assuming that the mixing ratio was constant as at the lowest aircraft altitude. For most spirals an SO<sub>2</sub> value from the surface was available to 'anchor' the profile, and it was found to be consistent with the constant mixing ratio scenario. In 5 flights, the integrated SO<sub>2</sub> was very close to the Pandora values with differences within 0.25 DU. The Pandora instrument was able to track the increase in VCD spanning 3 spirals, capturing the onset on August 23, 2013, of a large pollution event. On two occasions where the aircraft measurements showed near-zero SO<sub>2</sub> concentrations, Pandora's values were 0.12 DU and -0.2 DU, i.e., within the 1- $\sigma$  uncertainties of the measurements. Only for the final spiral was the aircraft VCD lower than the Pandora value by more than 0.6 DU. On that flight, both aircraft and Pandora data demonstrated elevated SO<sub>2</sub> values. The aircraft data showed a thin layer of SO<sub>2</sub> below 600 m with a maximum at 200 m (Figure 10). That may be an indication of the edge of the plume and the plume could be thicker along the Pandora optical path. Nevertheless, the average difference between the aircraft integrated values and Pandora VCDs was about 0.1 DU with the standard deviation of 0.38 DU or 0.27 DU if the last flight was excluded.

The Pandora SO<sub>2</sub> VCDs were also compared with measurements from the Dutch-Finnish Ozone Monitoring Instrument (OMI) on-board NASA Aura satellite (Levelt et al., 2006). The recent version based on the Principal Component Analysis algorithm (Li et al., 2013) with additional adjustment based on modelled SO<sub>2</sub> profiles over the oil sands region (McLinden et al., 2014) was used in this comparison. We also limited the comparison to pixel sizes under 40 km (track positions 11-50) centred within 15 km from Fort McKay. Only OMI measurements taken under snow-free and cloud-free



(cloud fraction  $<0.2$ ) conditions were used. The Pandora values were averaged within  $\pm 0.5$  hours from the OMI overpass time. A scatter plot of all 51 coincident OMI and Pandora measurements that satisfy these criteria is shown in Figure 12. The correlation coefficient between the two data sets is only about 0.2 and is not surprising given a large pixel size and high uncertainties of OMI measurements (0.5 DU at 1- $\sigma$  level) relative to the range of SO<sub>2</sub> levels. We simulated OMI and Pandora measurements using the EC GEM-MACH (Global Environmental Multi-scale – Modelling Air quality and Chemistry) (Makar et al., 2015a, 2015b) model at 2.5 km resolution, accounting for the size of the OMI pixel, the 15 km coincidence criteria, and considering the addition of realistic measurement noise. A detailed discussion of this simulation is outside the scope of this study, but we found that the correlation coefficient between such simulated Pandora and OMI data was only about 0.3. The model study indicates that the main culprits in the degradation of the correlation were the measurement noise (primarily in the OMI) and the OMI horizontal resolution. This example demonstrates that a simple “scatter plot” comparison of satellite and ground-based VCD measurements is not very informative and a proper account for satellite viewing geometry and measurement uncertainties is necessary.

## 5. Summary and Discussion

In order to study variability and changes of VCDs of major pollutants such as SO<sub>2</sub> in the Canadian oil sands region, a Pandora sunphotometer was installed at Fort McKay in August 2013. We found that the instrument is suitable for SO<sub>2</sub> monitoring and reliable enough to operate in remote areas. Originally, the instrument was deployed in a configuration with the instrument head mounted on a tripod and the spectrometer and computer installed in a water-proof plastic housing. In August 2014, the instrument spectrometer was redeployed with the spectrometer and computer installed indoors in a temperature-controlled environment and the instrument optical head connected by an optical cable, located on the roof of the instrument trailer. In this modified configuration, the instrument demonstrated that it can operate for extended periods under cold conditions.

The instrument is sensitive enough to measure anthropogenic SO<sub>2</sub> from two major SO<sub>2</sub> sources with total emissions of about 45 kt yr<sup>-1</sup> located approximately 20 km from the observation site. As expected, elevated VCD (up to 9 DU) and surface concentrations of SO<sub>2</sub> are observed when the wind is from the south and south-east, where the emission sources are located. With no industrial sources located to the west, VCD and surface concentrations are about zero for westerly winds.

The calibration procedure applied in this study was similar to that developed by Herman et al., (2009) for NO<sub>2</sub>, but it was modified to account for a much higher noise level of SO<sub>2</sub> VCD measurements (0.01 DU for NO<sub>2</sub> vs. 0.17 DU for SO<sub>2</sub>). This calibration procedure is based on the 25<sup>th</sup> (or 10<sup>th</sup>) percentile and makes the assumption that a sizable fraction of all measurements corresponds to SO<sub>2</sub>-free conditions. Fort McKay measurements stratified by the wind direction confirmed the validity of this approach: the average SO<sub>2</sub> values after the calibration procedure were close to zero for winds from the west where no SO<sub>2</sub> sources are found. This 25<sup>th</sup> (or 10<sup>th</sup>) percentile-based calibration approach is optimal when “clean” conditions occur frequently, e.g., for sites located in a vicinity of emission point sources where SO<sub>2</sub> VCDs depend on the wind direction.



However, lower percentiles such as the 10<sup>th</sup> or smaller may be required in regions with persistent high SO<sub>2</sub> values, e.g., in Eastern China.

Various sources of measurement uncertainties were examined. The statistical standard error of SO<sub>2</sub> VCD calculated by the spectral fitting algorithm is under 0.05 DU for 60% and under 0.15 DU for 90% of all direct sun observations. The instrument precision, calculated from parallel measurements by two instruments, is about 0.17 DU (1- $\sigma$ ). The spectral fitting procedure and the accuracy of the retrieved SO<sub>2</sub> values largely depend on properly accounting for ozone absorption and the reference spectrum. Based on some examples, we estimate that these factors can introduce errors up to 0.4 DU. Further development of the retrieval algorithms could improve the instrument accuracy. Measurements at Fort McKay, when the wind was from clean sectors, demonstrated that the overall Pandora uncertainty is under 0.26 DU (1- $\sigma$ ). The Pandora measurements were further validated using seven aircraft profile measurements that demonstrated a bias within 0.1 DU and the standard deviation of the difference under 0.3 DU for all but one of the aircraft profiles.

When used for satellite validation, simple “scatter plot” comparisons of coincident satellite and ground-based VCD measurements are less informative for a localized industrial source such as the oil sands and their interpretation requires a proper accounting of satellite viewing geometry and measurement uncertainties. The comparison of Pandora and OMI VCDs over Fort McKay demonstrated a low correlation, with a correlation coefficient of about 0.2. This is not surprising given a large pixel size, high uncertainties of OMI measurements (0.5 DU at 1- $\sigma$  level) relative to the range of SO<sub>2</sub> variations, and heterogeneity of the SO<sub>2</sub> spatial distribution at this location. The use of models to account for the difference in spatial and temporal resolution between ground-based and satellite measurements would greatly facilitate satellite SO<sub>2</sub> VCDs validation.

The comparison of SO<sub>2</sub> VCDs and surface concentrations at Fort McKay suggests that there is no simple link between these two characteristics. High surface concentrations contribute to the column values. A simple statistical relationship suggests that, on average, each 10 ppbv of surface concentration roughly correspond 1 DU of total column (similar to what one would calculate for 10 ppbv spread through a 1 km surface layer). However, elevated VCDs may be related to plumes that are above the ground with little or no fumigation and therefore may not produce elevated surface concentrations.

25

## Appendix 1

Information about the natural variability of measured parameter and measurement uncertainties can be derived from the measurements themselves. This approach known also as the Grubbs estimation method (Grubbs, 1948; Toohey and Strong, 2007) is often used to estimate the precision of measurements. For readers' convenience, we present the method here as it was described by (Fioletov et al., 2006).

The result of a measurement ( $M$ ) is the sum of the true measured value ( $X$ ) and an error ( $e$ ). Let us consider two instruments that measure the same parameter  $X$ , but with different errors  $e_1$  and  $e_2$ . The results of their measurements ( $M_1$  and  $M_2$ ) can be used to estimate the variances of  $X$ ,  $e_1$  and  $e_2$ , as follows: If we assume that the measured value and the errors are independent, then the variance of  $M$  is the sum of variances of  $X$  and  $e_i$ :



$$\sigma^2(M_i) = \sigma^2(X) + \sigma^2(e_i), \quad i=1,2. \quad (1)$$

The difference of  $M_1$  and  $M_2$  does not depend on  $X$ . If, in addition, we assume that the errors of different instruments are not correlated, then the variance of the difference is equal to the sum of  $\sigma^2(e_1)$  and  $\sigma^2(e_2)$ :

$$\sigma^2(M_1 - M_2) = \sigma^2(e_1) + \sigma^2(e_2) \quad (2)$$

5 The values of  $\sigma^2(M_1)$ ,  $\sigma^2(M_2)$ , and  $\sigma^2(M_1 - M_2)$  can be estimated from a set of parallel measurements. The three resulting equations can be solved for  $\sigma^2(X)$ ,  $\sigma^2(e_1)$ , and  $\sigma^2(e_2)$ :

$$\begin{aligned} \sigma^2(X) &= \frac{1}{2} (\sigma^2(M_1) + \sigma^2(M_2) - \sigma^2(M_1 - M_2)), \\ \sigma^2(e_1) &= \frac{1}{2} (\sigma^2(M_1) - \sigma^2(M_2) + \sigma^2(M_1 - M_2)), \\ \sigma^2(e_2) &= \frac{1}{2} (\sigma^2(M_2) - \sigma^2(M_1) + \sigma^2(M_1 - M_2)). \end{aligned} \quad (3)$$

10 Equations (3) were used to estimate the standard deviation (SD) of instrument errors (we will refer to it as to standard instrument uncertainty) and the SD of variability.

In the reality, we do not actually know the variances  $\sigma^2(M_i)$  and  $\sigma^2(M_1 - M_2)$ ; we can only estimate them, with a certain error, from the available measurements. The  $\alpha$ -level confidence interval for the variance  $\sigma^2$  depends on the estimated variance value itself and the number of data points,  $n$ :

$$15 \quad \frac{(n-1)s^2}{\chi^2_{1-\alpha/2}(n-1)} < \sigma^2 < \frac{(n-1)s^2}{\chi^2_{\alpha/2}(n-1)} \quad (4)$$

where  $s^2$  is the sample variance and  $\chi^2(n-1)$  is the chi-square distribution with  $n-1$  degrees of freedom. The error of the variance estimate depends on the variance itself. All three variances,  $\sigma^2(M_1)$ ,  $\sigma^2(M_2)$ , and  $\sigma^2(M_1 - M_2)$ , determine  $\sigma^2(X)$ ,  $\sigma^2(e_1)$ , and  $\sigma^2(e_2)$  in (3). Therefore, the errors in the  $\sigma^2(X)$ ,  $\sigma^2(e_1)$ , and  $\sigma^2(e_2)$  estimates depend on the sum of all three variances  $\sigma^2(M_1)$ ,  $\sigma^2(M_2)$ , and  $\sigma^2(M_1 - M_2)$ , and can be high even if the estimated variance itself is low (but one or more of the variances  $\sigma^2(M_1)$ ,  $\sigma^2(M_2)$ , or  $\sigma^2(M_1 - M_2)$  are high). The estimates are thus only as accurate as the least accurate of these parameters. The variance estimates can be improved by increasing the number of data points.

**Acknowledgments.** The authors wish to thank the NRC-FRL flight crew of the Convair 580 for making the airborne study possible. Funding for the airborne study over the oil sands region was provided in part by Environment Canada's Clean Air  
 25 Regulatory Agenda (CARA). We acknowledge the NASA Earth Science Division for funding of OMI SO<sub>2</sub> product development and analysis. The Dutch - Finnish built OMI instrument is part of the NASA's EOS Aura satellite payload. We thank systems engineering, instrument calibration and satellite integration teams for making this mission a success. The OMI project is managed by KNMI and the Netherlands Agency for Aero-space Programs (NIVR).



## References

- De Backer, H. and Muer, D. De: Intercomparison of total ozone data measured with Dobson and Brewer spectrophotometers at Uccle (Belgium) from January 1984 to March 1991, including zenith sky observations, *J. Geophys. Res.*, 96, 20,711–20,719, 1991.
- Bais, A. F., Zerefos, C. S., Meleti, C., Ziomas, I. C. and Tourpali, K.: Spectral measurements of solar UVB radiation and its relation to total ozone, SO<sub>2</sub>, and clouds, *J. Geophys. Res.*, 98, 5199–5204, 1993.
- Carn, S. A., Krotkov, N. A., Yang, K. and Krueger, A. J.: Measuring global volcanic degassing with the Ozone Monitoring Instrument (OMI), *Geol. Soc. London, Spec. Publ.*, 380(1), 229–257, doi:10.1144/SP380.12, 2013.
- 10 Carn, S. A., Krueger, A. J., Bluth, G. S. J., Schaefer, S. J., Krotkov, N. A., Watson, I. M. and Datta, S.: Volcanic eruption detection by the Total Ozone Mapping Spectrometer (TOMS) instruments: A 22-year record of sulfur dioxide and ash emissions, in *Volcanic Degassing*, Special Publication of the Geological Society of London, edited by C. Oppenheimer, D. M. Pyle, and J. Barclay, pp. 177–202, Geological Society, London, UK., 2003.
- Carn, S. A., Krueger, A. J., Krotkov, N. A., Yang, K. and Levelt, P. F.: Sulfur dioxide emissions from Peruvian copper smelters 15 detected by the Ozone Monitoring Instrument, *Geophys. Res. Lett.*, 34(9), L09801, doi:10.1029/2006GL029020, 2007.
- Clarisse, L., Fromm, M., Ngadi, Y., Emmons, L., Clerbaux, C., Hurtmans, D. and Coheur, P.-F.: Intercontinental transport of anthropogenic sulfur dioxide and other pollutants: An infrared remote sensing case study, *Geophys. Res. Lett.*, 38(19), L19806, doi:10.1029/2011GL048976, 2011.
- 20 Eisinger, M. and Burrows, J. P.: Tropospheric sulfur dioxide observed by the ERS-2 GOME instrument, *Geophys. Res. Lett.*, 25(22), 4177–4180, 1998.
- Fioletov, V. E., Griffioen, E., Kerr, J. B., Wardle, D. I. and Uchino, O.: Influence of volcanic sulfur dioxide on spectral UV irradiance as measured by Brewer Spectrophotometers, *Geophys. Res. Lett.*, 25(10), 1665–1668, doi:10.1029/98GL51305, 1998.
- 25 Fioletov, V. E., McLinden, C. A., Krotkov, N., Moran, M. D. and Yang, K.: Estimation of SO<sub>2</sub> emissions using OMI retrievals, *Geophys. Res. Lett.*, 38(21), L21811, doi:10.1029/2011GL049402, 2011.
- Fioletov, V. E., McLinden, C. A., Krotkov, N., Yang, K., Loyola, D. G., Valks, P., Theys, N., Van Roozendaal, M., Nowlan, C. R., Chance, K., Liu, X., Lee, C. and Martin, R. V.: Application of OMI, SCIAMACHY, and GOME-2 satellite SO<sub>2</sub> retrievals for detection of large emission sources, *J. Geophys. Res. Atmos.*, 118(19), 11,399–11,418, 30 doi:10.1002/jgrd.50826, 2013.
- Fioletov, V. E., Tarasick, D. W. and Petropavlovskikh, I.: Estimating ozone variability and instrument uncertainties from SBUV(2), ozonesonde, Umkehr, and SAGE II measurements: Short-term variations, *J. Geophys. Res.*, 111(D2), D02305, doi:10.1029/2005JD006340, 2006.



- De Foy, B., Krotkov, N. A., Bei, N., Herndon, S. C., Huey, L. G., Martínez, A. P., Ruiz-Suárez, L. G., Wood, E. C., Zavala, M., Molina, L. T. and Mart, A.: Hit from both sides: Tracking industrial and volcanic plumes in Mexico City with surface measurements and OMI SO<sub>2</sub> retrievals during the MILAGRO field campaign, *Atmos. Chem. Phys.*, 9(24), 9599–9617, 2009.
- 5 Galle, B., Johansson, M., Rivera, C., Zhang, Y., Kihlman, M., Kern, C., Lehmann, T., Platt, U., Arellano, S. and Hidalgo, S.: Network for Observation of Volcanic and Atmospheric Change (NOVAC)—A global network for volcanic gas monitoring: Network layout and instrument description, *J. Geophys. Res.*, 115(D5), D05304, doi:10.1029/2009JD011823, 2010.
- Georgoulias, A. K., Balis, D., Koukouli, M. E., Meleti, C., Bais, A. and Zerefos, C.: A study of the total atmospheric sulfur dioxide load using ground-based measurements and the satellite derived Sulfur Dioxide Index, *Atmos. Environ.*, 43(9), 1693–1701, doi:10.1016/j.atmosenv.2008.12.012, 2009.
- 10 Gordon, M., Li, S.-M., Staebler, R., Darlington, A., Hayden, K., O'Brien, J. and Wolde, M.: Determining air pollutant emission rates based on mass balance using airborne measurement data over the Alberta oil sands operations, *Atmos. Meas. Tech.*, 8(9), 3745–3765, doi:10.5194/amt-8-3745-2015, 2015.
- 15 Grubbs, F. E.: On estimating precision of measuring instruments and product variability, *J. Am. Stat. Assoc.*, 242, 243–264, 1948.
- Herman, J., Cede, A., Spinei, E., Mount, G., Tzortziou, M. and Abuhassan, N.: NO<sub>2</sub> column amounts from ground-based Pandora and MFDOAS spectrometers using the direct-sun DOAS technique: Intercomparisons and application to OMI validation, *J. Geophys. Res.*, 114(D13), D13307, doi:10.1029/2009JD011848, 2009.
- 20 Herman, J., Evans, R., Cede, A., Abuhassan, N., Petropavlovskikh, I. and McConville, G.: Comparison of ozone retrievals from the Pandora spectrometer system and Dobson spectrophotometer in Boulder, Colorado, *Atmos. Meas. Tech. Discuss.*, 8(3), 3049–3085, doi:10.5194/amtd-8-3049-2015, 2015.
- Hutchinson, T. C. and Whitby, L. M.: The effects of acid rainfall and heavy metal particulates on a boreal Forest ecosystem near the sudbury smelting region of Canada, *Water. Air. Soil Pollut.*, 7(4), 421–438, doi:10.1007/BF00285542, 1977.
- 25 Kelly, E. N., Schindler, D. W., Hodson, P. V., Short, J. W., Radmanovich, R. and Nielsen, C. C.: Oil sands development contributes elements toxic at low concentrations to the Athabasca River and its tributaries., *Proc. Natl. Acad. Sci. U. S. A.*, 107(37), 16178–83, doi:10.1073/pnas.1008754107, 2010.
- Kerr, J. B.: New methodology for deriving total ozone and other atmospheric variables from Brewer spectrophotometer direct sun spectra, *J. Geophys. Res.*, 107(D23), 4731, doi:10.1029/2001JD001227, 2002.
- 30 Kerr, J. B., Asbridge, I. A. and Evans, W. F. J.: Intercomparison of total ozone measured by the Brewer and Dobson spectrophotometers at Toronto, *J. Geophys. Res.*, 93, 11129–11140, doi:10.1029/JD093iD09p11129, 1988.
- Knepp, T., Pippin, M., Crawford, J., Chen, G., Szykman, J., Long, R., Cowen, L., Cede, a., Abuhassan, N., Herman, J., Delgado, R., Compton, J., Berkoff, T., Fishman, J., Martins, D., Stauffer, R., Thompson, a. M., Weinheimer, a., Knapp, D., Montzka, D., Lenschow, D. and Neil, D.: Estimating surface NO<sub>2</sub> and SO<sub>2</sub> mixing ratios from fast-





- response total column observations and potential application to geostationary missions, *J. Atmos. Chem.*, (2), doi:10.1007/s10874-013-9257-6, 2013.
- Koenker, R. and Bassett, G. W.: Regression Quantiles, *Econometrica*, 46, 33–50, 1978.
- Krueger, A. J., Schaefer, S. J., Krotkov, N., Bluth, G. and Barker, S.: Ultraviolet remote sensing of volcanic emissions, in  
5 Remote Sensing of Active Volcanism, vol. 116, edited by M. Mougini and J. Crisp, pp. 25–43, American Geophysical Union., 2000.
- Krueger, A. J., Walter, L. S., Bhartia, P. K., Schnetzler, C. C., Krotkov, N. A., Sprod, I. and Bluth, G. J. S.: Volcanic sulfur dioxide measurements from the Total Ozone Mapping Spectrometer instruments, *J. Geophys. Res.*, 100(D7), 14057–14076, doi:10.1029/95JD01222, 1995.
- 10 Lee, C., Martin, R. V., Van Donkelaar, A., Lee, H., Dickerson, R. R., Hains, J. C., Krotkov, N., Richter, A., Vinnikov, K. and Schwab, J. J.: SO<sub>2</sub> emissions and lifetimes: Estimates from inverse modeling using in situ and global, space-based (SCIAMACHY and OMI) observations, *J. Geophys. Res.*, 116(D6), D06304, doi:10.1029/2010JD014758, 2011.
- Levelt, P. F., van den Oord, G. H. J., Dobber, M. R., Malkki, A., Stammes, P., Lundell, J. O. V. and Saari, H.: The Ozone Monitoring Instrument, *IEEE Trans. Geosci. Remote Sens.*, 44(5), 1093–1101, doi:10.1109/TGRS.2006.872333,  
15 2006.
- Li, C., Joiner, J., Krotkov, N. A. and Bhartia, P. K.: A fast and sensitive new satellite SO<sub>2</sub> retrieval algorithm based on principal component analysis: Application to the ozone monitoring instrument, *Geophys. Res. Lett.*, 40(23), 6314–6318, doi:10.1002/2013GL058134, 2013.
- Longo, B. M., Yang, W., Green, J. B., Crosby, F. L. and Crosby, V. L.: Acute health effects associated with exposure to  
20 volcanic air pollution (vog) from increased activity at Kilauea Volcano in 2008., *J. Toxicol. Environ. Health. A*, 73(20), 1370–81, doi:10.1080/15287394.2010.497440, 2010.
- Makar, P. A., Gong, W., Hogrefe, C., Zhang, Y., Curci, G., Zabkar, R., Milbrandt, J., Im, U., Balzarini, A., Baro, R., Bianconi, R., Cheung, P., Forkel, R., Gravel, S., Hirtl, H., Honzak, L., Hou, A., Jimenez-Guerrero, P., Langer, M., Moran, M. D., Pabla, B., Perez, J. L., Pirovano, G., San Jose, R., Tuccella, P., Werhahn, J., Zhang, J. and Galmarini, S.:  
25 Feedbacks between air pollution and weather, part 2: Effects on chemistry, *Atmos. Environ.*, 115, 499–526, doi:doi:10.1016/j.atmosenv.2014.10.021, 2015a.
- Makar, P. A., Gong, W., Milbrandt, J., Hogrefe, C., Zhang, Y., Curci, G., Zabkar, R., Im, U., Balzarini, A., Baro, R., Bianconi, R., Cheung, P., Forkel, R., Gravel, S., Hirtl, H., Honzak, L., Hou, A., Jimenez-Guerrero, P., Langer, M., Moran, M. D., Pabla, B., Perez, J. L., Pirovano, G., San Jose, R., Tuccella, P., Werhahn, J., Zhang, J. and Galmarini, S.:  
30 Feedbacks between air pollution and weather, part 1: Effects on weather, *Atmos. Environ.*, 115, 442–469, doi:doi:10.1016/j.atmosenv.2014.12.003, 2015b.
- McLinden, C. A., Fioletov, V., Boersma, K. F., Kharol, S. K., Krotkov, N., Lamsal, L., Makar, P. A., Martin, R. V., Veefkind, J. P. and Yang, K.: Improved satellite retrievals of NO<sub>2</sub> and SO<sub>2</sub> over the Canadian oil sands and comparisons with surface measurements, *Atmos. Chem. Phys.*, 14(7), 3637–3656, doi:10.5194/acp-14-3637-2014, 2014.



- McLinden, C. A., Fioletov, V., Boersma, K. F., Krotkov, N., Sioris, C. E., Veefkind, J. P. and Yang, K.: Air quality over the Canadian oil sands: A first assessment using satellite observations, *Geophys. Res. Lett.*, 39(4), 1–8, doi:10.1029/2011GL050273, 2012.
- McLinden, C., Fioletov, V., Krotkov, N. A., Li, C., Boersma, K. F. and Adams, C.: A decade of change in NO<sub>2</sub> and SO<sub>2</sub> over the Canadian oil sands as seen from space., *Environ. Sci. Technol.*, doi:10.1021/acs.est.5b04985, 2015.
- Nowlan, C. R., Liu, X., Chance, K., Cai, Z., Kurosu, T. P., Lee, C. and Martin, R. V.: Retrievals of sulfur dioxide from the Global Ozone Monitoring Experiment 2 (GOME-2) using an optimal estimation approach: Algorithm and initial validation, *J. Geophys. Res.*, 116(D18), D18301, doi:10.1029/2011JD015808, 2011.
- Platt, U. and Stutz, J.: *Differential Optical Absorption Spectroscopy*, Springer, Berlin, Heidelberg., 2008.
- Pope, C. A. and Dockery, D. W.: Health effects of fine particulate air pollution: Lines that connect, *J. Air Waste Manag. Assoc.*, 56(6), 709–742, 2006.
- Reed, A. J., Thompson, A. M., Kollonige, D. E., Martins, D. K., Tzortziou, M. A., Herman, J. R., Berkoff, T. A., Abuhassan, N. K. and Cede, A.: Effects of local meteorology and aerosols on ozone and nitrogen dioxide retrievals from OMI and Pandora spectrometers in Maryland, USA during DISCOVER-AQ 2011, *J. Atmos. Chem.*, doi:10.1007/s10874-013-9254-9, 2013.
- Richter, A., Weber, M., Burrows, J. P., Lambert, J.-C. and van Gijssel, A.: Validation strategy for satellite observations of tropospheric reactive gases, *Ann. Geophys.*, 56, 1–10, doi:10.4401/ag-6335, 2013.
- Rix, M., Valks, P., Hao, N., Loyola, D., Schlager, H., Huntrieser, H., Flemming, J., Koehler, U., Schumann, U. and Inness, A.: Volcanic SO<sub>2</sub>, BrO and plume height estimations using GOME-2 satellite measurements during the eruption of Eyjafjallajökull in May 2010, *J. Geophys. Res. Atmos.*, 117, doi:10.1029/2011JD016718, 2012.
- Simpson, I. J., Blake, N. J., Barletta, B., Diskin, G. S., Fuelberg, H. E., Gorham, K., Huey, L. G., Meinardi, S., Rowland, F. S., Vay, S. A., Weinheimer, A. J., Yang, M. and Blake, D. R.: Characterization of trace gases measured over Alberta oil sands mining operations: 76 speciated C<sub>2</sub>–C<sub>10</sub> volatile organic compounds (VOCs), CO<sub>2</sub>, CH<sub>4</sub>, CO, NO, NO<sub>2</sub>, NO<sub>y</sub>, O<sub>3</sub> and SO<sub>2</sub>, *Atmos. Chem. Phys.*, 10(23), 11931–11954, doi:10.5194/acp-10-11931-2010, 2010.
- Theys, N., Champion, R., Clarisse, L., Brenot, H., van Gent, J., Dils, B., Corradini, S., Merucci, L., Coheur, P.-F., Van Roozendael, M., Hurtmans, D., Clerbaux, C., Tait, S. and Ferrucci, F.: Volcanic SO<sub>2</sub> fluxes derived from satellite data: a survey using OMI, GOME-2, IASI and MODIS, *Atmos. Chem. Phys.*, 13(12), 5945–5968, doi:10.5194/acp-13-5945-2013, 2013.
- Thomas, W., Erbetseder, T., Ruppert, T., Roozendael, M. Van, Verdebout, J., Balis, D., Meleti, C. and Zerefos, C.: On the retrieval of volcanic sulfur dioxide emissions from GOME backscatter measurements, *J. Atmos. Chem.*, 50(3), 295–320, doi:10.1007/s10874-005-5544-1, 2005.
- Toohey, M. and Strong, K.: Estimating biases and error variances through the comparison of coincident satellite measurements, *J. Geophys. Res. Atmos.*, 112(D13), 1–12, doi:Artn D13306\|rDoi 10.1029/2006jd008192, 2007.



- Tzortziou, M., Herman, J. R., Cede, A. and Abuhassan, N.: High precision, absolute total column ozone measurements from the Pandora spectrometer system: Comparisons with data from a Brewer double monochromator and Aura OMI, *J. Geophys. Res.*, 117(D16), D16303, doi:10.1029/2012JD017814, 2012.
- 5 Tzortziou, M., Herman, J. R., Cede, A., Loughner, C. P., Abuhassan, N. and Naik, S.: Spatial and temporal variability of ozone and nitrogen dioxide over a major urban estuarine ecosystem, *J. Atmos. Chem.*, doi:10.1007/s10874-013-9255-8, 2013.
- Vandaele, A. C., Simon, P. C., Guilmot, J. M., Carleer, M. and Colin, R.: SO<sub>2</sub> absorption cross section measurement in the UV using a Fourier transform spectrometer, *J. Geophys. Res.*, 99(D12), 25599–25605, 1994.
- 10 Wang, T., Hendrick, F., Wang, P., Tang, G., Clémer, K., Yu, H., Fayt, C., Hermans, C., Gielen, C., Müller, J.-F., Pinardi, G., Theys, N., Brenot, H. and Van Roozendaal, M.: Evaluation of tropospheric SO<sub>2</sub> retrieved from MAX-DOAS measurements in Xianghe, China, *Atmos. Chem. Phys.*, 14(20), 11149–11164, doi:10.5194/acp-14-11149-2014, 2014.
- Wood, J.: *Environmental Policy Indicators — Air Quality*, Studies in Environmental Policy, Fraser Institute., 2012.
- 15 Wu, F. C., Xie, P. H., Li, A., Chan, K. L., Hartl, A., Wang, Y., Si, F. Q., Zeng, Y., Qin, M., Xu, J., Liu, J. G., Liu, W. Q. and Wenig, M.: Observations of SO<sub>2</sub> and NO<sub>2</sub> by mobile DOAS in the Guangzhou eastern area during the Asian Games 2010, *Atmos. Meas. Tech.*, 6(9), 2277–2292, doi:10.5194/amt-6-2277-2013, 2013.
- Zerefos, C., Ganev, K., Kourtidis, K., Tzortziou, M., Vasaras, A. and Syrakov, E.: On the origin of SO<sub>2</sub> above Northern Greece, *Geophys. Res. Lett.*, 27(3), 365–368, doi:10.1029/1999GL010799, 2000.



**Table 1.** SO<sub>2</sub> VCD calculated from measurements of seven aircraft flights, from Pandora 104 measurements and surface SO<sub>2</sub> concentrations.

Date and time (MST)	Min. aircraft VCD (DU)	Max. aircraft VCD (DU)	Pandora VCD (DU)	Surface (ppbv)
23 Aug 2013 10:49	0.04	0.04	0.16	0.16
23 Aug 2013 12:20	0.63	0.77	0.38	5.93
23 Aug 2013 13:59	1.08	1.31	1.10	9.49
24 Aug 2013 11:28	0.18	0.30	0.27	3.04
24 Aug 2013 13:04	0.15	0.28	0.72	9.36
02 Sep 2013 10:36	0.02	0.02	-0.21	
03 Sep 2013 16:09	0.26	0.39	1.06	



**Figure 1.** Pandora instruments at Fort McKay in (left) 2013 and (right) 2014-2015. In 2013, the instruments head was installed on a white Brewer tripod and the spectrometer and computer were inside the black box to the right. From 2014, the head was installed on the roof of a trailer with the spectrometer and computer located inside the trailer.

5

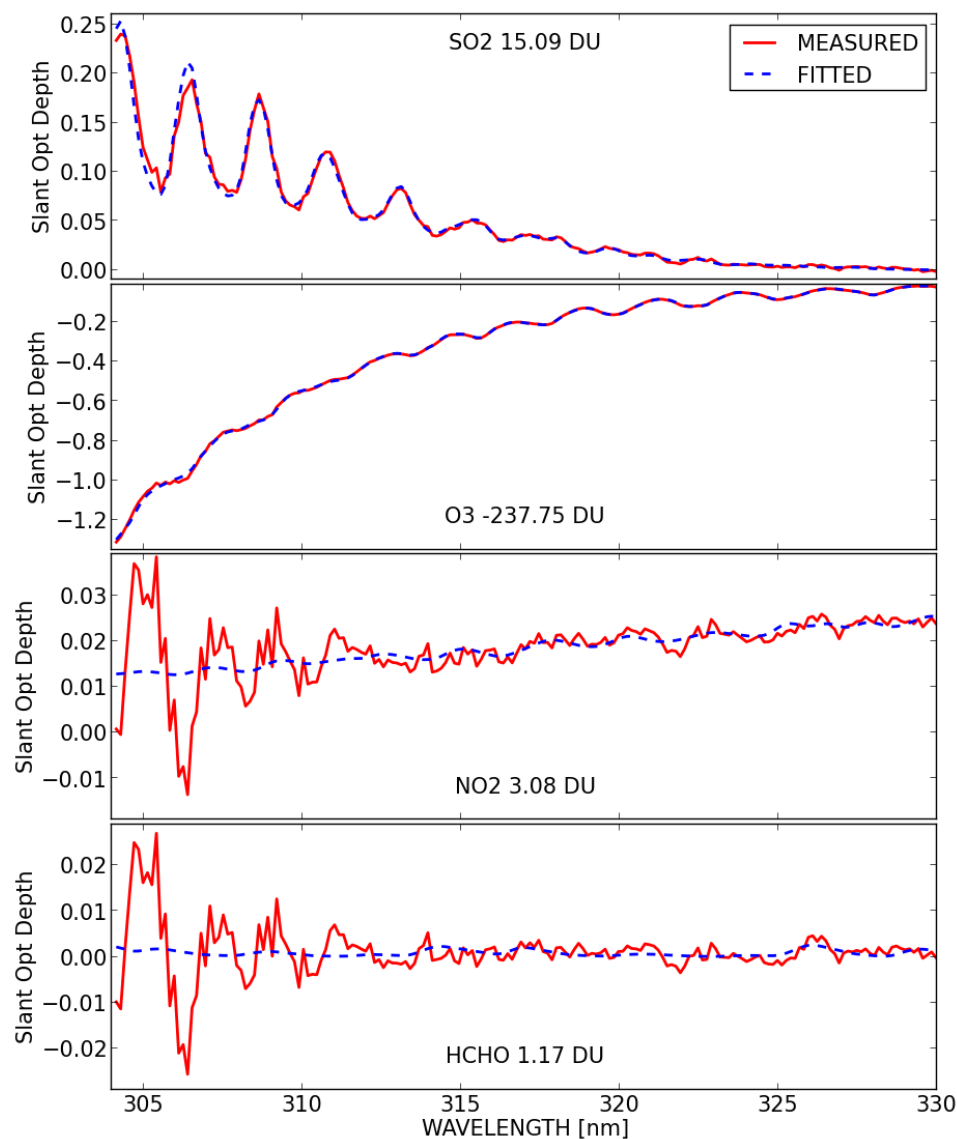


**Figure 2.** Fitted Pandora slant column optical depths (blue) for a measurement at Fort McKay on August 2, 2015 at 07:42 MST (red) when some of the highest  $\text{SO}_2$  values were observed. The synthetic reference spectrum was used in the fitting (see text for details). The negative  $\text{O}_3$  slant column means that there was more  $\text{O}_3$  in the reference than in the measurements at 07:42 MST. Note that  $\text{NO}_2$  and  $\text{HCHO}$  are fitted in this fitting windows, but only to improve the results for  $\text{SO}_2$ .

5



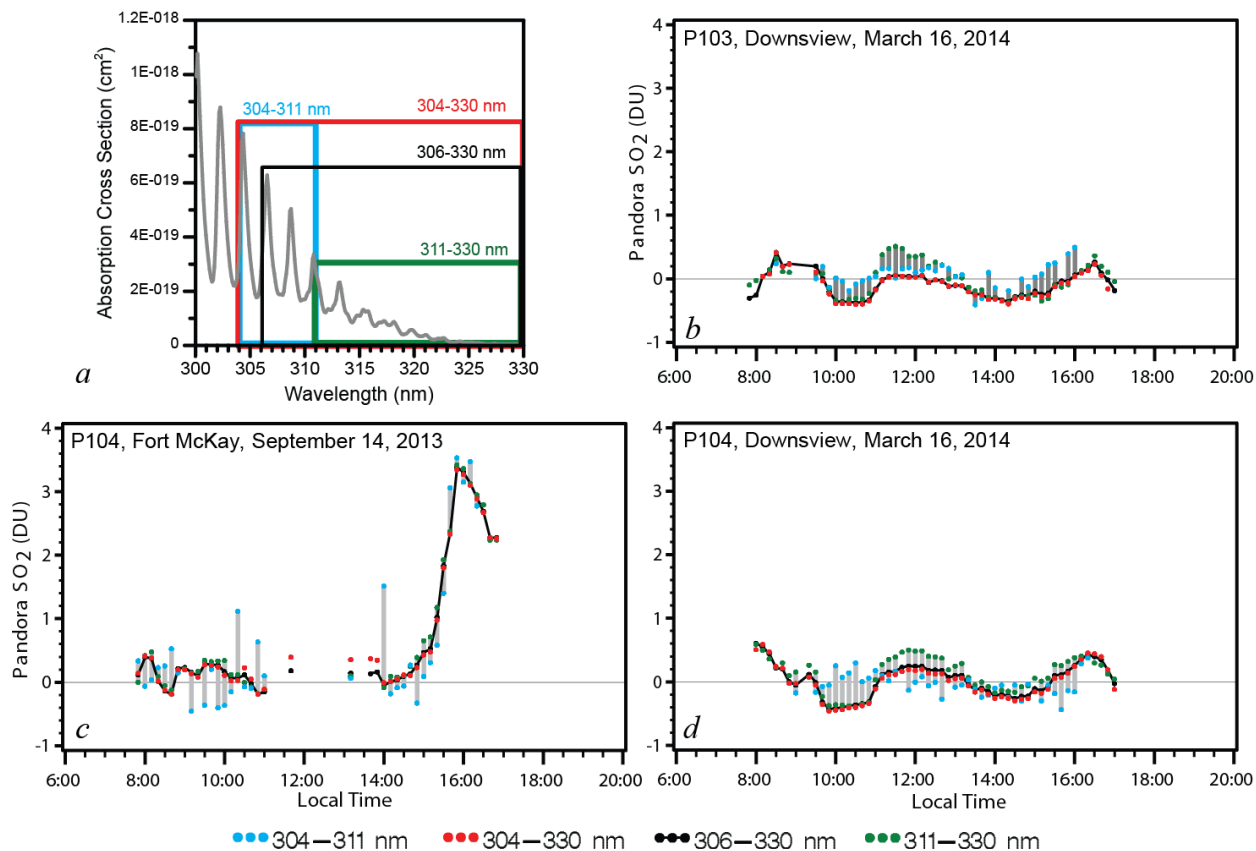


**Figure 3.** Examples of SO<sub>2</sub> VCD retrieved using different spectral windows as indicated on the plot. Data are from Pandora 104 at Fort McKay, September 14, 2013, and Downsview, March 16, 2014, are shown. Different colors represent different spectral windows used for the fitting. Grey bars connect SO<sub>2</sub> values retrieved from 304-311 and 311-330 nm spectral windows.

5

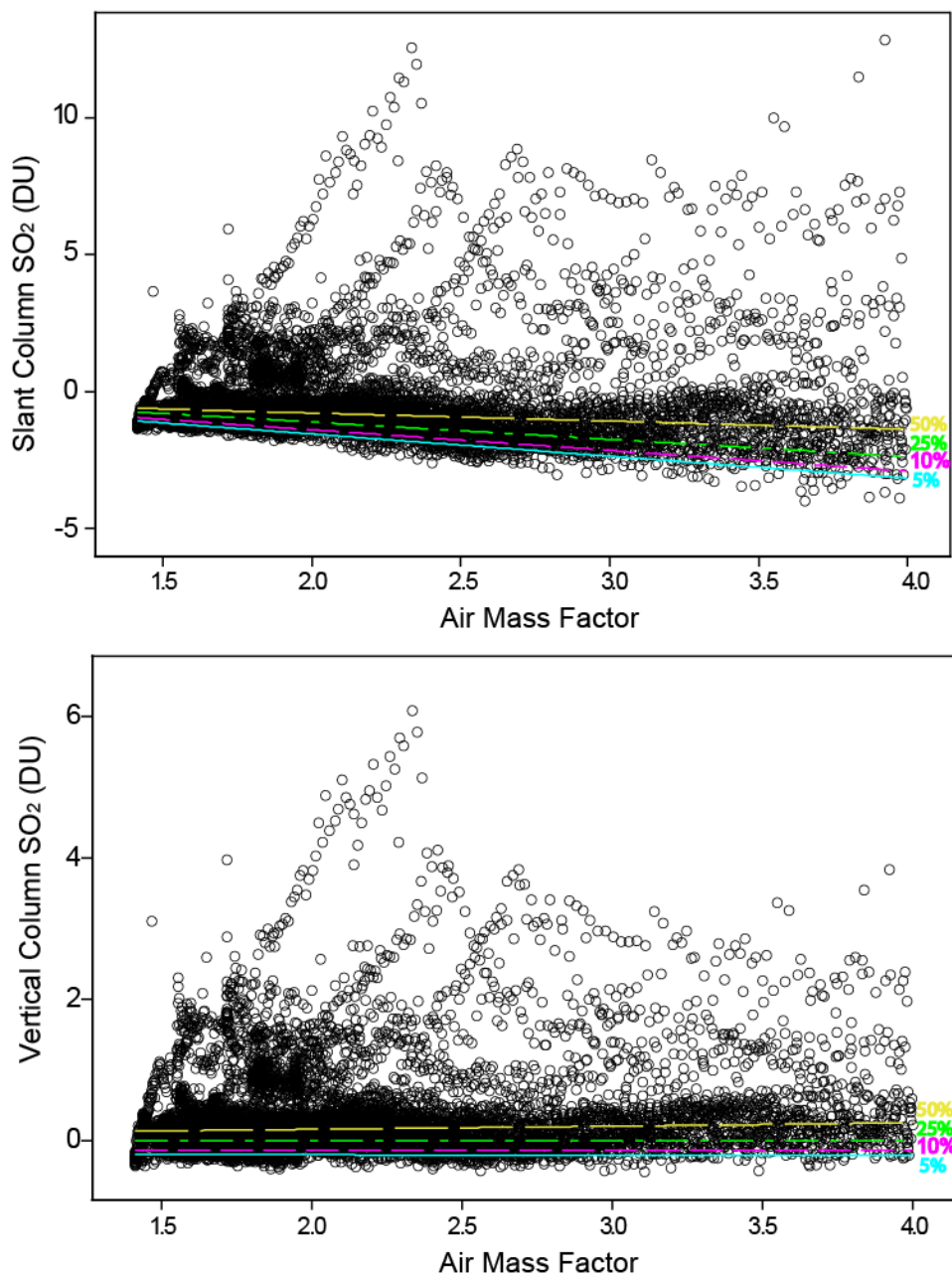


**Figure 4.** (top) Slant column densities derived from 306-330 nm spectral fitting of Pandora 103 data at Fort McKay in August 2013. (bottom) Vertical column densities derived from the same data using the fit based on 25<sup>th</sup> percentile (see text for details). The lines corresponding to 5<sup>th</sup>, 10<sup>th</sup>, 25<sup>th</sup>, and 50<sup>th</sup> percentiles are also shown.

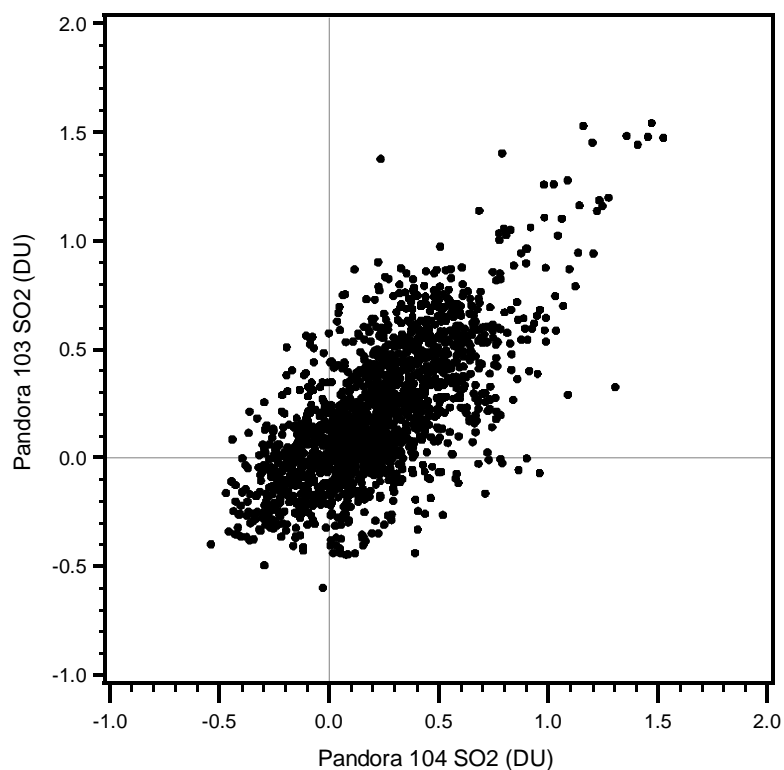


**Figure 5.** The scatter plot of coincidental SO<sub>2</sub> measurements at Downsview by Pandora 103 and 104 in January-July 2014. The data were grouped into 10-minute bins and only bins with between 5 and 7 individual measurements were used for the comparison. The total number of bins was 1844. The correlation coefficient between the plotted data is 0.7.

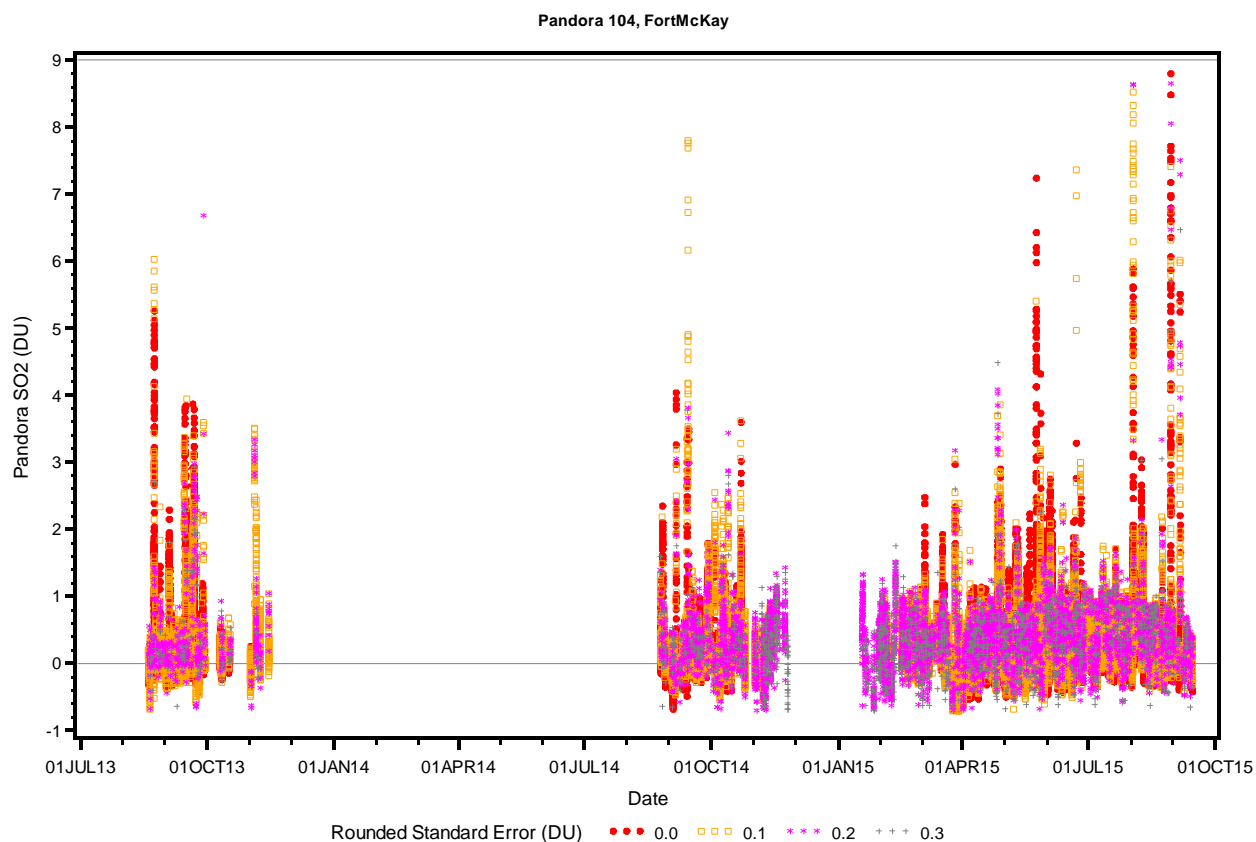


**Figure 6.** Time series of SO<sub>2</sub> measurements at Fort McKay from August 2013 to October 2015. Different symbols and colours represent different standard errors estimated by the fitting algorithm. Data from December 2014 – January 2015 are missing because of low Sun elevation ( $\mu > 5$ ).

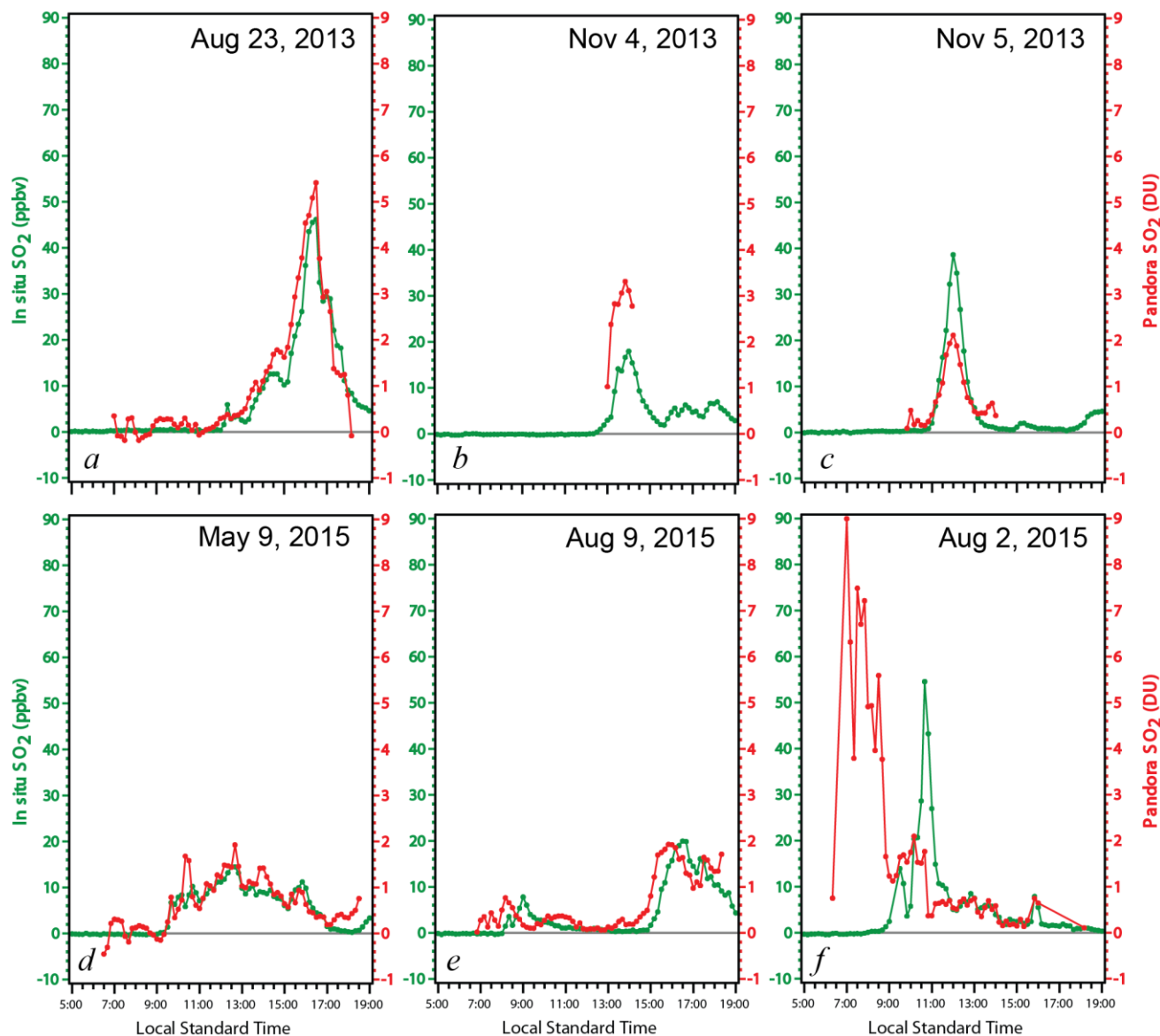


**Figure 7.** Vertical Column Density (DU) measured by Pandora spectrometer at Fort McKay and in situ  $\text{SO}_2$  concentration (ppbv) measured at the same location for 6 days that illustrate fluctuations of VCDs and surface concentrations. Note that the vertical scales are the same on all 6 plots.

5

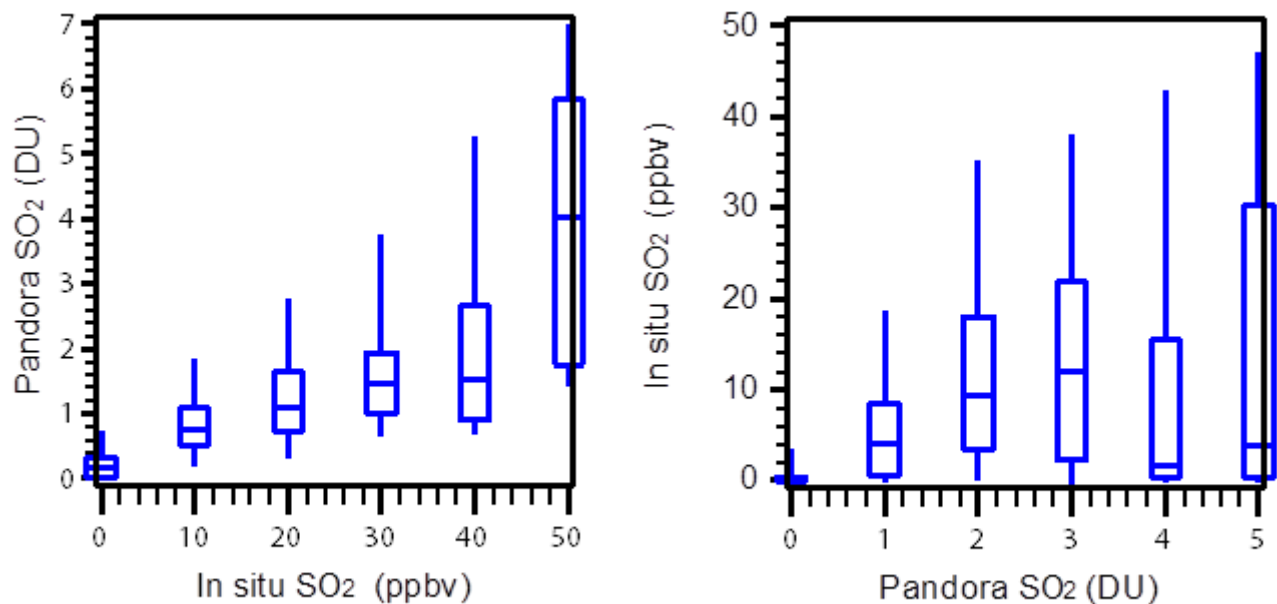


**Figure 8.** VCD and surface concentration SO<sub>2</sub> data binned by (left) surface concentration and (right) VCD values. Binned VCD and surface concentration data show a clear link between the two parameters, but binning by Pandora's values gives a different result from the binning by in situ data. When the surface concentration is elevated, vertical columns are also elevated. However, in about 25% cases, surface concentrations are close to zero even when the vertical column values are elevated. The bottom and top edges of the box are located at the sample 25<sup>th</sup> and 75<sup>th</sup> percentiles, the whiskers correspond to the 5<sup>th</sup> and 95<sup>th</sup> percentiles. The centre horizontal line is drawn at the median.

5



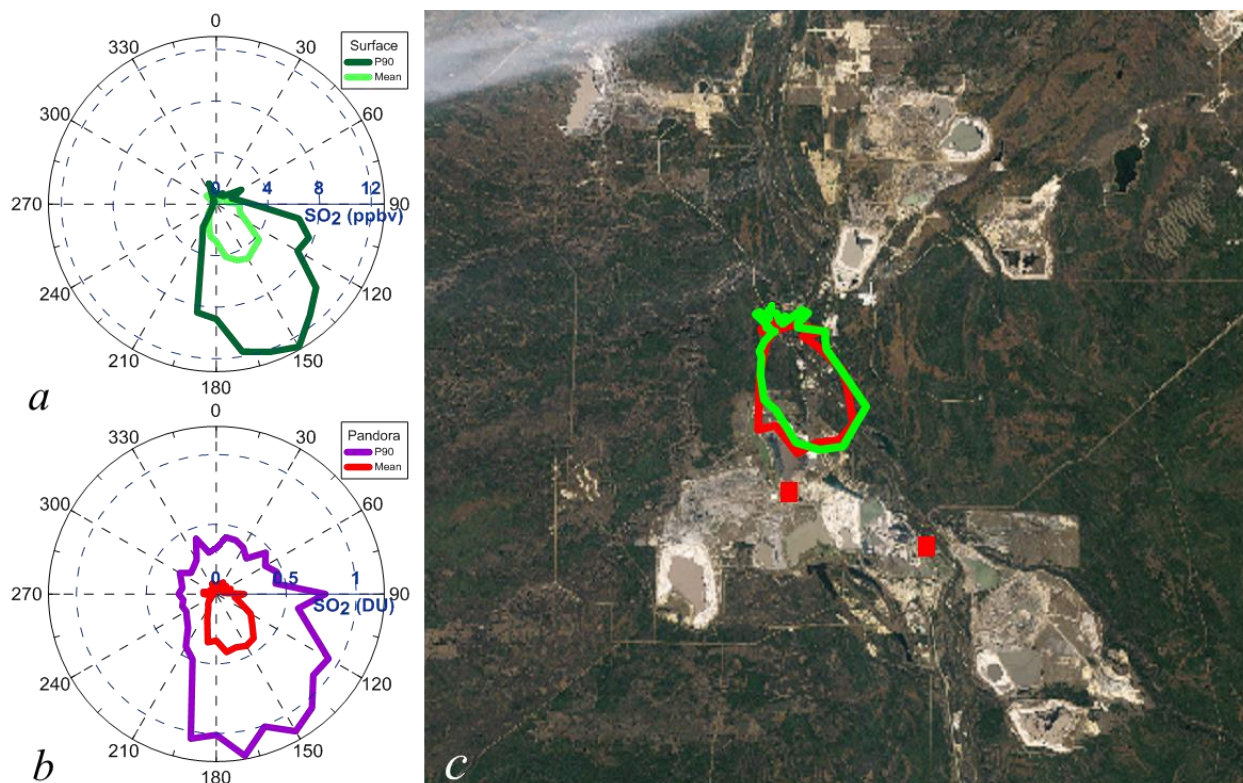


**Figure 9.** The mean and 90th percentile of in situ SO<sub>2</sub> concentration (a) and Pandora SO<sub>2</sub> VCD (b) at Fort McKay as a function of the wind direction in 2013–2015. Both Pandora and in-situ data shows similar patterns: high SO<sub>2</sub> values are associated with south-east winds (c) The mean values from the plots (a) and (b) overlaid with Landsat images of the surface mining area (<http://earthobservatory.nasa.gov/Features/WorldOfChange/athabasca.php?all=y>). The plots are based on only coincide Pandora and in situ measurements averaged over 10-minute intervals. The two red squares indicate the major SO<sub>2</sub> emission sources. Data for this plot were binned into 10-degree bins by the wind direction.

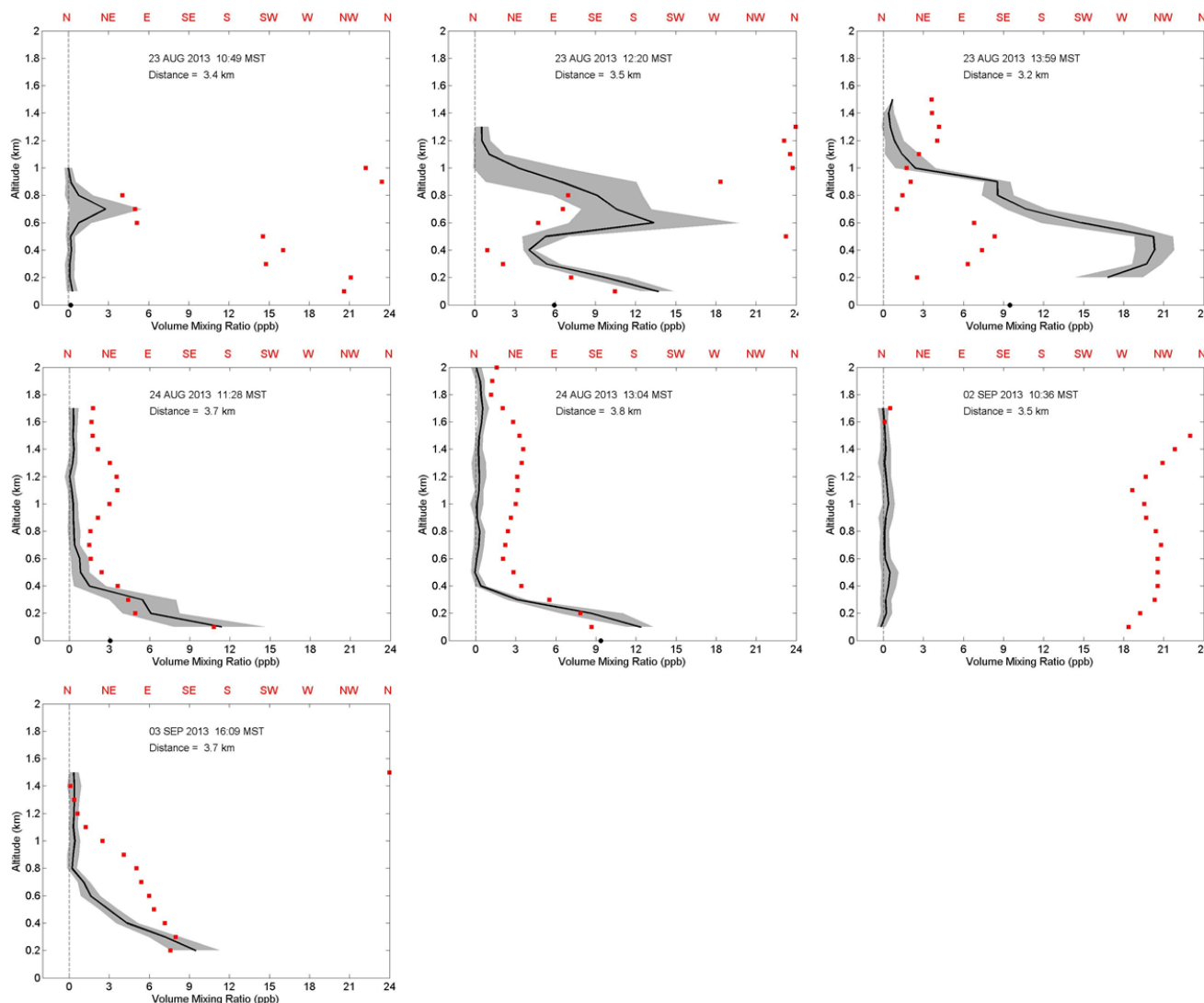
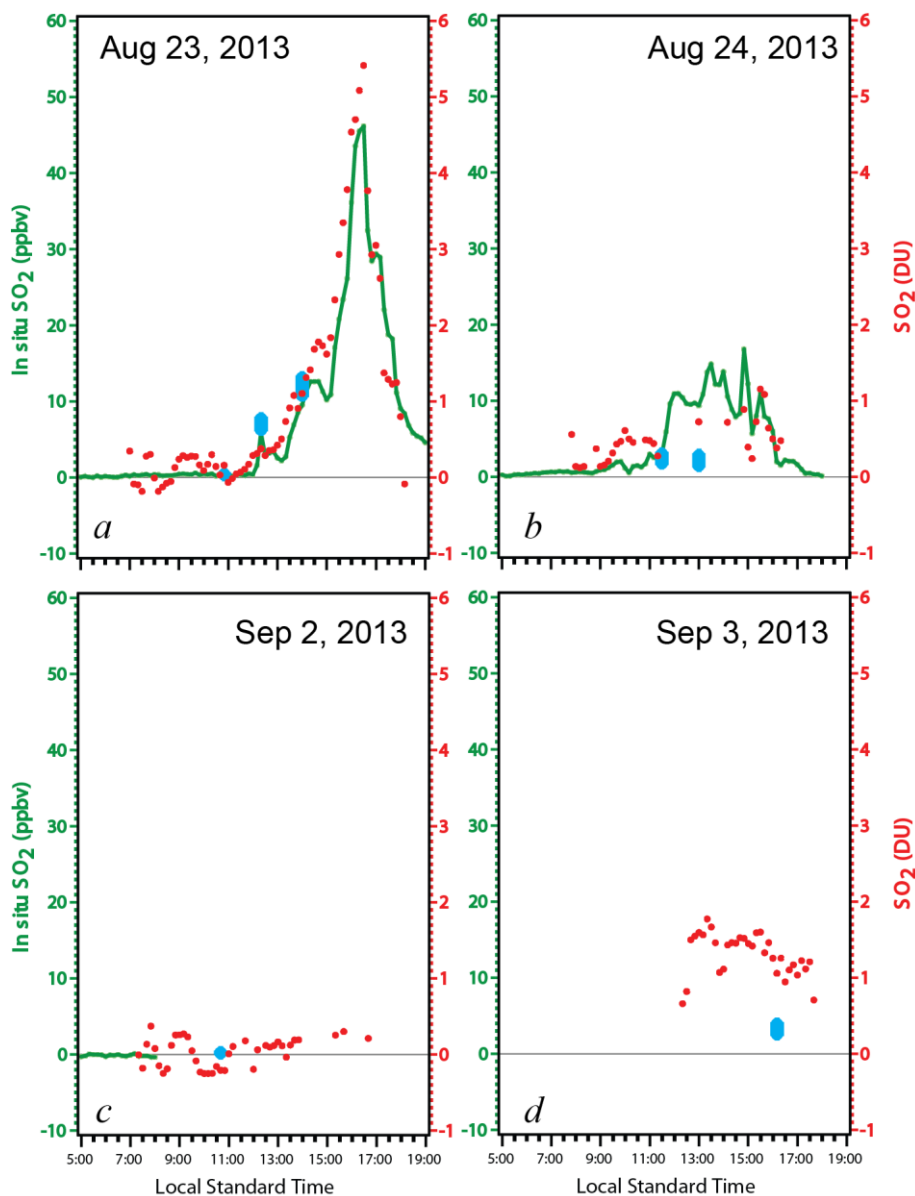


**Figure 10.** The measured vertical profiles of  $\text{SO}_2$  mixing ratios in ppbv (the black lines) with  $1-\sigma$  uncertainties as a function of altitude for 7 spiral flight around Fort McKay in August-September 2013. The black dots indicate mixing ratios at the surface. The red dots represent the wind directions as labelled on the top axis. Note that the two major  $\text{SO}_2$  sources are located and south-south east of Fort McKay. The dates and times of the flights and the mean distances from Fort McKay are also shown.

5



5 **Figure 11.** SO<sub>2</sub> VCD (DU) measured by Pandora spectrometer (red) at Fort McKay and calculated from integrated aircraft SO<sub>2</sub> profile measurements (blue), as well as in situ SO<sub>2</sub> concentration in ppbv (green). The vertical blue bars represent the range of SO<sub>2</sub> VCDs calculated from two assumptions: for 0 mixing below the lowest aircraft flight height and a constant mixing ratio that corresponds to the missing ratio at the lowest altitude where SO<sub>2</sub> was measured.

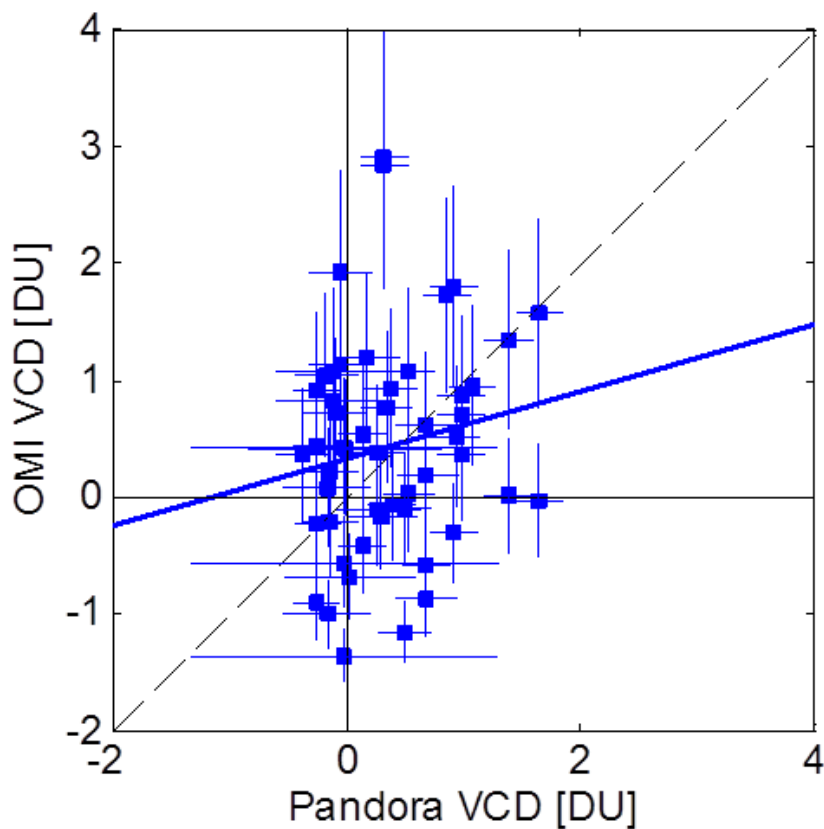


**Figure 12.** A scatter plot of  $\text{SO}_2$  VCD values measured by the OMI satellite instrument and Pandora. The correlation coefficient between the two data sets is 0.17 and the slope of the regression line is 0.23. The error bars represent  $2\text{-}\sigma$  intervals.